Antiviral Research 219 (2023) 105733

Contents lists available at ScienceDirect

Antiviral Research

journal homepage: www.elsevier.com/locate/antiviral

Intermittent therapy with helicase-primase inhibitor IM-250 efficiently controls recurrent herpes disease and reduces reactivation of latent HSV

David I. Bernstein [a], Nancy M. Sawtell [a], Fernando J. Bravo [a], David A. Dixon [a], Christian Gege [b], Gerald Kleymann [b,*]

[a] Cincinnati Children's Hospital Medical Center (CCHMC), University of Cincinnati, OH, USA
[b] Innovative Molecules GmbH, Lipowsky Str. 10, 81373, Munich, Bavaria, Germany

ARTICLE INFO

Keywords:
Herpes simplex virus
HSV
Antiviral
Therapy
Treatment
Helicase-primase inhibitor
HPI
IM-250
Latency
Recurrence
Latent virus
Cure

ABSTRACT

Herpes is a contagious life-long infection with persistently high incidence and prevalence, causing significant disease worldwide. Current therapies have efficacy against active HSV infections but no impact on the latent viral reservoir in neurons. Thus, despite treatment, disease recurs from latency and the infectious potential remains unaffected within patients.

Here, efficacy of the helicase-primase inhibitor (HPI) IM-250 against chronic neuronal HSV infections utilizing two classic herpes *in vivo* latency/reactivation animal models (intravaginal guinea pig HSV-2 infection model and ocular mouse HSV-1 infection model) is presented. Intermittent therapy of infected animals with 4–7 cycles of IM-250 during latency silences subsequent recurrences analyzed up to 6 months. In contrast to common experience, our studies show that the latent reservoir is indeed accessible to antiviral therapy altering the latent viral reservoir such that reactivation frequency can be reduced significantly by prior IM-250 treatment.

We provide evidence that antiviral treatment during HSV latency can reduce future reactivation from the latent reservoir, supporting a conceptual shift in the antiviral field, and reframing what is achievable with respect to therapy of latent neuronal HSV infections.

1. Introduction

Infection with herpes simplex viruses (HSV) type 1 and type 2 are common. Worldwide HSV-2 prevalence is 13%, which can increase to over 85% of populations in Sub-Saharan Africa. HSV-1 infections are even more common with 66.6% global prevalence, by 49 years of age (James et al., 2020). Once infected, HSV persists for life as a latent neuronal infection that can reactivate to cause recurrent disease or recurrent shedding without lesions. HSV infections are the cause of herpes labialis (cold sores), genital herpes, sight-impairing disease (keratitis), and, less frequently, life-threatening disease mainly in immunocompromised patients, including transplant patients and newborns. HSV infections of the central nervous system (CNS) including the brain (encephalitis) are especially difficult to treat because CNS penetration of the therapeutic agent is required.

The most widely used treatment for HSV infections over the last 4 decades have been the nucleoside analogues that currently include acyclovir, valacyclovir, and famciclovir (Kleymann, 2005; De Clercq and Li, 2016; Workowski and Bolan, 2015). During treatment these drugs can effectively reduce the frequency of recurrences and virus shedding but only partially effect transmission (Corey et al., 2004). Drug resistance is uncommon in immunocompetent persons but occurs in immunocompromised hosts (Bacon et al., 2003). Therefore, alternative agents to treat HSV infections are needed. More recently, helicase-primase inhibitors (HPIs), like amenamevir, have been approved in Japan for VZV in 2017 and HSV in 2024 (Kawashima et al., 2023) and pritelivir, evaluated in clinical trials for therapy of genital herpes (Wald et al., 2014) and now in Phase 3 clinical trials for ACV-resistant/foscarnet intolerable HSV infections in immunocompromised patients. Importantly, none of these therapies have an effect after therapy is discontinued and there is no evidence that they effect the burden of persistent, latent virus when used after latency is established (Bryson et al., 1983; Wald et al., 1994); what many would consider the holy grail of HSV therapy.

IM-250 is a HPI with fewer of off-target activities or toxicities compared to previous candidates (Gege et al., 2021; Uhlig et al., 2021).

* Corresponding author.
E-mail address: gerald.kleymann@innovativemolecules.com (G. Kleymann).

https://doi.org/10.1016/j.antiviral.2023.105733
Received 25 August 2023; Received in revised form 13 October 2023; Accepted 13 October 2023
Available online 18 October 2023

In addition, IM-250 has, uniquely, sufficient target tissue penetration, including CNS, to offer distinct advantages over other HPIs (Gege et al., 2021). Previous studies of IM-250 therapy in guinea pigs suggested that the latent viral reservoir was reduced compared to vehicle control or acyclovir (ACV) treatment (Gege et al., 2021). However, the number of animals evaluated was small and therapy may not have been optimal. Therefore, to further investigate this intriguing observation, we designed studies that included larger numbers of animals, prolonged therapy and increased the number of endpoints to include viral genome copy number and explant reactivation. In addition, we extended our studies to include the mouse ocular model. This model of induced *in vivo* reactivation allowed us to evaluate whether IM-250 treatment, when restricted to specific *timed* reactivation events, would alter the reactivation competency of the latent reservoir subsequent to the intermittent treatments. These new studies offer strong evidence that IM-250 affects the pool of neurons responsible for most reactivation events, reframing what is achievable with respect to treatment of persistent latent HSV infections.

2. Materials and methods

2.1. Cells and viruses

Cells: Rabbit skin cells (RSCs) were originally obtained from B. Roizman at the University of Chicago, while Vero (CCL-81) cells were obtained from ATCC. Both were maintained and propagated according to ATCC protocols.

Virus: HSV-2 strain MS (ATCC-VR540) was grown in low passage primary rabbit kidney cells and titered on Vero cell monolayers (Bourne et al., 2000). HSV-1 strain 17VP16placZ was constructed from strain 17syn+ (original source: John Subak-Sharpe). This virus contains a lytic marker, specifically, the VP16 promoter driving the *E. coli* β-galactosidase (LacZ) gene. 17VP16placZ replicates like wild type 17syn+ *in vitro* and *in vivo*. The details of construction and characterization of this virus has been reported previously (Sawtell and Thompson, 2016, 2020). It was replicated in RSCs and titered on RSC monolayers.

2.2. Antivirals

Acylovir (ACV, Sigma Co., St. Louis, MO) was obtained from the Cincinnati Children's Medical Center pharmacy and dissolved in sterile saline solution for *ad libitum* administration (5 mg/ml) to animals in drinking water (Bernstein et al., 2015). The HPI IM-250 was produced according to published patents (Kleymann and Gege, 2017, 2019). IM-250 was provided in PS guinea pig chow V2233 *ad libitum* (at either 500 mg/kg in diet carrier [high dose chow, ~15 mg/kg/day IM-250] or 150 mg/kg in diet carrier [low dose diet, ~5 mg/kg/day IM-250]). For mouse experiments, IM-250 was provided in mouse chow V1124 (150 mg/kg in diet carrier, ~5 mg/kg/day IM-250) *ad libitum*. Both guinea pig and mouse chow vehicle and IM-250 containing diet was formulated by ssniff Spezialdiäten GmbH, Germany. For oral gavage in mice, IM-250 was prepared just before use by dissolving in sterile DMSO followed by further dilution in PBS containing 0.5% hydroxypropyl methylcellulose (HPMC, Sigma Aldrich) and ultrasonic processing for 5 min (Gege et al., 2021; Uhlig et al., 2021). A gastric needle was utilized to deliver 200 μl of IM-250 (10 mg/kg) or vehicle as detailed (Uhlig et al., 2021).

2.3. Animals

All procedures were reviewed and approved by the CCHMC Institutional Animal Care and Use Committee and comply with NIH guidelines. Animals were housed in American Association for Laboratory Animal Care (AALAC)-approved facilities.

50 female Hartley guinea pigs (250–350 g) were obtained from Charles River Breeding Laboratories (Wilmington, MA). 100 Swiss Webster (SW) outbred mice (strain #: Hsd:ND4) 22–25 g were obtained from Envigo (Frederick Maryland).

2.4. Intravaginal guinea pig HSV-2 infection model

Female Hartley guinea pigs were inoculated intravaginally with 1×10^6 pfu of HSV-2 (MS strain) by instilling 0.1 ml of a virus suspension into the vaginal vault (Bernstein, 2020).

As in humans, virus then reactivates to cause recurrent lesions in the genital area. Treatment was initiated at 21 days after infection and given intermittently at weekly intervals for 12 weeks by providing drugs in the animal chow (IM-250) or drinking water (ACV). Recurrent disease was determined from days 25–183 when the animals were sacrificed. The total amount of latent HSV was then determined by qPCR and reactivatable virus by explant cocultivation.

Primary genital skin disease was quantified using a lesion score-scale ranging from 0 representing no disease to 4 representing severe vesiculoulcerative skin disease of the perineum (Stanberry et al., 1982). After recovery from primary disease (day 21) animals were randomly assigned to intermittent treatment with IM-250, ACV or vehicle (no treatment) ($n = 18$) based on primary disease scores. Animals without evidence of acute disease or a positive swab sample 2 days after inoculation were not included in the study. Intermittent treatments included either 7 days of IM-250 chow, ACV in the drinking water (Bernstein et al., 2015), or no treatment followed by 7 days of vehicle chow or plain water for 7 days for the IM-250 and ACV groups, respectively. The dose of *ad libitum* ACV was estimated at 150–250 mg/kg/day. Intermittent therapy was chosen because prior experience suggested this was superior to continued therapy for prolonged effects on recurrent disease (Gege et al., 2021). Animals were then examined 5 days a week (Mon-Fri) from day 25–183 days post-infection for evidence of spontaneous recurrent herpetic lesions (Bernstein, 2020; Stanberry et al., 1982). The number of lesion days (days on which a recurrent lesion was observed on the perineum) was recorded. Three days after the final treatment, the guinea pigs were sacrificed, and the dorsal root ganglia (DRG) from the lumbo sacral area and spinal cords (SC) were harvested aseptically. The tissues were then divided and approximately half used to perform explant evaluations (Stanberry et al., 1982) and half for qPCR.

2.4.1. Detection of latent virus by qPCR HSV-2 DNA

Viral DNA levels in neural tissues were determined as previously described (Bernstein et al., 2020). In brief, the DRGs and SC were homogenized on ice and DNA was extracted from tissue homogenate using the QIAamp DNA Mini Kit (Qiagen #51306) according to the manufacturer's protocol. The eluted DNA was quantified using a Nanodrop 2000 spectrophotometer and equal amounts of DNA were used to perform quantitative PCR using an Applied Biosystems 7500 Fast Real-Time PCR System.

To determine the levels of HSV-2 DNA in neural tissue, HSV-2 gG2 gene detection was performed by quantitative PCR (Bernstein et al., 2015). The gG2 primer and probe sequences were as follows:

Forward: 5′-CGG/AGA/CAT/TCG/AGT/ACC/AGA/TC-3′; reverse: 5′-GCC/CAC/CTC/TAC/CCA/CAA/CA-3′; and probe: 5′-FAM-ACC/CAC/GTG/CAG/CTC/GCC/G-tamRA-3′.

Each PCR reaction contained 100 ng of DNA, 0.5 μM of each primer, 0.10 μM of FAM/tamRA fluorescent probe, and 10 μl of Taqman Gene Expression Master Mix (ABI) in a total volume of 20 μl reaction. PCR amplification was performed on a 7500 Fast Real-Time PCR system (ABI). Using the following conditions: pre-incubation at 50 °C for 2 min and 95 °C for 10 min followed by 40 cycles consisting of a denaturation step at 95 °C for 15 s, annealing at 60 °C for 1 min, and elongation at 72 °C for 10 s. A standard curve for each virus was generated with ten-fold serial dilutions of purified HSV-2 DNA (ATCC) containing 10^5–10^0 HSV-2 copies in 50 ng of uninfected guinea pig brain DNA. The limit of detection was determined to be 5 HSV genome copies, with excellent

linearity ($R \geq 0.98$) over 5 logs of HSV genomic DNA content.

2.4.2. Guinea pig explant

The lumbosacral dorsal root ganglia and spinal cord were removed, minced, and explanted onto Vero cells. Each sample provided one culture for the DRG and 5 for the SC. Explant cultures were observed for 21 days for evidence of an HSV-induced cytopathic effect with media changes every 7 days. After 21 days, supernatants from wells without evidence of reactivation were re-cultured on fresh cells for another 7 days.

2.5. Ocular mouse HSV-1 infection model

The effect of intermittent IM-250 treatment on the reactivation competency of the latent viral reservoir was evaluated in the mouse ocular model (Sawtell and Thompson, 2021). In this model, viral latency is established in the trigeminal ganglia (TG) and hyperthermic stress (HS) is utilized to induce *in vivo* reactivation in the TG where the number of neurons exiting latency is quantified at the individual cell level (Sawtell and Thompson, 1992; Sawtell, 1998, 2003, 2005). Male Swiss Webster (Envigo) mice were anesthetized prior to inoculation by intraperitoneal injection of sodium pentobarbital in sterile saline (50 mg/kg of body weight). Anesthetized mice were infected by dispensing 10 μL of inoculum containing 1–2x10^5 pfu of HSV-1 strain 17VP16pLacZ onto each scarified corneal surface (Sawtell and Thompson, 1992).

2.6. IM-250 therapy of latently infected mice

Infected mice were maintained for 45 days to ensure establishment of latency. Mice were then randomized into two groups. In experiment 1, IM-250 (10 mg/kg) or vehicle was administered by oral gavage 3 h prior to hyperthermic stress (HS). At 24 h post HS, animals were sacrificed and reactivation in the TG was quantified by two methods, firstly a sensitive assay to detect directly the infectious virus produced in the TG during the reactivation event, secondly an assay to detect viral lytic cycle activity and proteins in individual neurons undergoing reactivation. This assay evaluates the reactivation competency of the viral genomes latent in the TG.

In experiment 2, mice were placed on IM-250 (150 mg/kg in diet carrier, ~5 mg/kg/day IM-250) or vehicle diet intermittently as shown (Fig. 5). A total of 4 on/off cycles were carried out over 70 days. Reactivation was induced by HS at the midpoint of each treatment cycle. A final HS in the absence of treatment was carried out 13 days after IM-250 withdrawal. 24 h after this final HS, neurons undergoing reactivation were quantified, thereby directly evaluating the reactivation competency of the latent reservoir.

2.7. In vivo reactivation

Latent HSV was induced to reactivate *in vivo* using a single HS per cycle (Sawtell and Thompson, 1992). In brief, each mouse was placed in a restrainer and suspended in a 42.5–42.8 °C water bath for 10 min. Mice were subsequently towel dried and placed in a 35 °C incubator for 20–30 min to prevent hypothermia.

2.8. Infectious virus reactivation assay

TG were homogenized on ice in 1 ml straight-walled Radnoti homogenizers. Cell debris was separated by centrifugation and supernatant dispensed onto RSC monolayer and overlayed with 0.1% carboxymethyl cellulose to prevent spread. At 48–72 h RSC were rinsed, stained with crystal violet and plaques counted using a dissecting microscope.

2.9. Histochemistry and immunohistochemistry

In situ detection of HSV lytic cycle in whole TG was carried out using a dual staining method as detailed previously (Sawtell and Thompson, 2020). The infecting viral strain, 17VP16pLacZ, expresses β-galactosidase when the VP16 promoter is active. This leaky late promoter is silenced during latency and thus the activation of this promoter coincides with activation of the viral lytic cycle (Thompson et al., 2009). Viral proteins are restricted to the lytic cycle and are not expressed during latency. Dual detection of these two lytic markers first utilizes a standard x-gal assay followed by whole ganglia immunohistochemistry. The primary rabbit anti-HSV antibody (Accurate, AXL237) was detected by the secondary HRP labeled goat anti-rabbit antibody (Vector). Color development was achieved by exposing ganglia to a 0.1 M Tris (pH 8.2) solution containing 250 μg of diaminobenzidine (Aldrich)/ml and 0.004% H_2O_2. Ganglia were cleared in glycerol and pressed between slides. Post processing for histology after whole ganglion histo- and immunohistochemistry has been recently detailed (Doll et al., 2020). Neuronal counts were performed on slides of 8 μm sectioned TG stained with cresyl violet. Equal numbers of TG were sampled for each group and the same number of fields were counted for each group. All slides were viewed under an Olympus BX40 microscope (manual operation) fitted with Olympus Uplan FL 4X/0.10, 10X/0.30, 20X/0.5, 40X/0.75, and 100X/1.25 oil objectives and photographed with Axio-CamHRc using Axiovision software (Zeiss). Two blinded microscopists independently viewed and counted neurons.

2.10. Bioanalytical measurements

Drug plasma concentrations of selected infected guinea pigs ($n = 6$ per group) and uninfected pharmacokinetic animals ($n = 3$ per group) were determined. Plasma samples of infected guinea pigs were collected in the morning (~10 a.m.) on the last day of the first treatment cycle (day 27 post infection, 7th day of therapy), while plasma samples of pharmacokinetic animals fed on the same schedule as the infected animals were collected on days 1, 2, 3, 5, 7, 8, 9, 10, 12, 14 at 10 a.m. and analyzed for drug exposure.

IM-250 and acyclovir plasma concentrations were quantified in animal plasma samples using liquid chromatography with tandem mass spectrometric detection (LC-MS/MS) d3-IM-250 as internal standard. Plasma (20 μl) was extracted with 2 vol of acetonitrile by vigorous shaking and subsequent centrifugation (8870×*g*, 10 min). The supernatant was diluted with water 1:1 (v:v) before injection (2 μl). Analytes were separated on a High Performance Liquid Chromatography apparatus from Thermo Fisher Scientific equipped with an analytical column (Aeris Widepore XB-C8) using an acetonitrile + 0.2% HFBA (heptafluorobutyric acid, eluent A)/0.2% HFBA gradient in water (eluent B), pump flow rate: 500 μl/min. The gradient (%B) was as follows: 0–0.1 min 95%; 2.2–4.0 min 3%; 4.1–5.7 min 95%. The retention times were 0.87 min for acyclovir and 3.07 min for IM-250. Mass spectrometry was performed on a Q Exactive Plus (Orbitrap) accurate mass spectrometer equipped with a heated electrospray (H-ESI) interface (positive PRM mode). The calibration standards were prepared in the following concentrations: 2.4, 7.2, 28.8, 120, 720, 2160, 6000, 12000, 28800 ng/mL in plasma.

2.11. Statistical analysis

Study size calculation for the animal experiments were based on suggestions by a statistician and many years of experience with these models. In general, the number of animals per group was chosen to ensure that we have approximately 80% power to detect a difference of about 50% comparing the main outcome for treated to untreated animals.

For comparison of the means for two groups a Student's *t*-test was performed using two-tailed analysis. For comparison of multiple groups, an ANOVA was initially performed and if significant differences among all the groups was noted, a Tukey's test to adjust for multiple comparisons was used. Data are presented as means and standard deviations.

Incidence data were compared by Fisher's exact test. A P value < 0.05 was considered significant.

3. Results

3.1. Pharmacokinetics and safety

To correlate the dose response with plasma exposure in experimental animals, drug plasma concentrations of infected guinea pigs and uninfected pharmacokinetic animals were determined.

3.1.1. Pharmacokinetics and safety in guinea pigs

The mean plasma concentration of infected mice of vehicle, IM-250 (500 mg/kg in diet) and ACV (5 mg/ml in drinking water) treated groups were 0.0, 12.3 ± 4.0 and 3.0 ± 1.5 μM (day 27 post infection, 7th day of treatment 10 a.m.), and this is well above the reported IC_{50} values for IM-250 (Gege et al., 2021) and somewhat above the IC_{50} for acyclovir. In a parallel pharmacokinetic study of uninfected guinea pigs

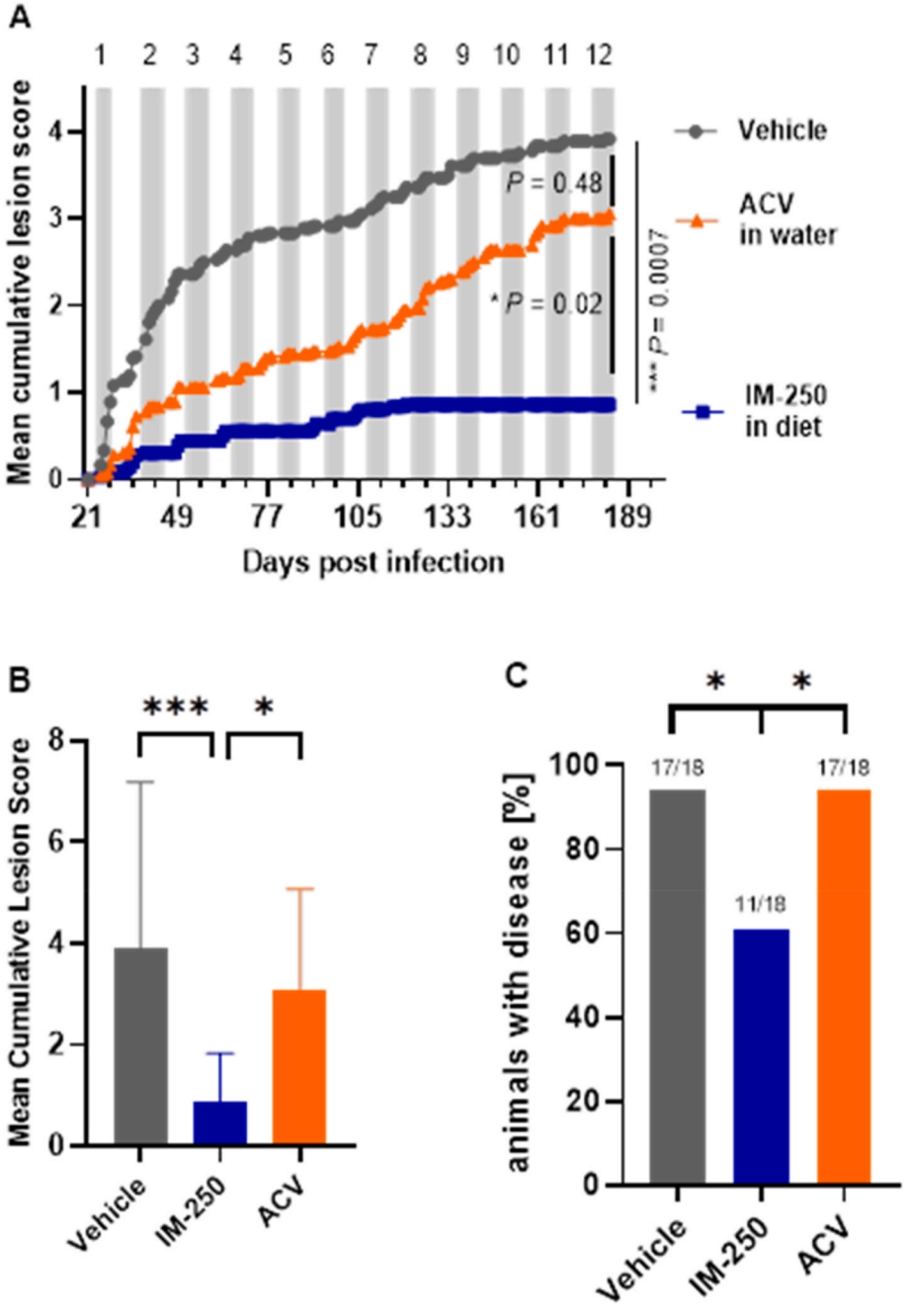

Fig. 1. Effect of therapies on recurrent disease.
HSV-2 infected guinea pigs (n = 18/per group) were randomized after latency was established (day 21) to receive twelve cycles of 7 days on and off therapy (over 6 months). IM-250 was administered by diet and ACV was added to drinking water, respectively, along with a vehicle group. (**A**) Mean cumulative recurrent lesion scores over the entire observation period (gray bars with cycle numbers at the top indicate treatment periods). To calculate the cumulative mean lesion score, the group's mean lesion score for each day starting at day 21 is calculated and added to the previous day scores until the end of the study. (**B**) Comparison of mean lesion scores over the entire observation period (days 25–181) shows significant reduction of lesion score of IM-250 treated group versus Vehicle (***$P < 0.001$) or ACV treated groups (*$P < 0.05$). Multiple comparison of groups was performed by ANOVA adjusted by Tukey's test. (**C**) Significantly fewer animals developed recurrent lesions over the entire period in the IM-250 treated group versus Vehicle (*$P < 0.05$) or ACV treated groups (*$P < 0.05$).

($n = 3$), fed with the 150 mg/kg IM-250 containing diet for 7 days, the mean total plasma IM-250 concentrations were 2.5, 3.1, 3.3, 3.5 and 3.3 μM on day 1, 2, 3, 5 and 7 at 10 a.m., respectively. After the 7 days of therapy (by changing the diet to standard chow) the plasma concentrations of IM-250 dropped to 1.0, 0.3, 0.08 and 0.007 μM on days 8, 9, 10 and 12 at 10 a.m., respectively. Thus, after 48 h the plasma concentration of IM-250 was below the IC_{50} of ~1 μM, if the high protein binding *in vivo* is considered (Gege et al., 2021, Fig. S1). Since the off treatment period was analyzed starting after the weekends (>48 h), no effects are anticipated to be caused by residual drug.

At the end of the first 7 days of treatment, the animals treated with high dose IM-250 guinea pig chow had a net average weight loss of 42.3 g (438.9 ± 23.5 g) when compared to the no treatment group (513.4 ± 50.6 g) and the ACV treated group (526.5 ± 57.2 g, $P < 0.0001$). These animals recovered their weight during the following 9-day period of vehicle only chow. Most likely the high concentration of IM-250 in the chow was less palatable to the animals, since the exposure in animals is above the IC_{50}, but well below the NOAEL (Gege et al., 2021), e.g. no weight loss was observed for guinea pigs at 13–26 μM plasma exposure during 20 mg/kg/day oral dosing with IM-250 (Gege et al., 2021, Fig. 4D). However, to avoid further weight loss, a new treatment regimen consisting of high dose IM-250, for the initial 2 days of the 7-day treatment period, followed by the lower dose administered for the remaining 5 days of the 7-day treatment period, was used. This provided a loading dose followed by a well-tolerated follow-up similar to that used in the human trial of pritelivir (Wald et al., 2014).

3.1.2. Pharmacokinetics and safety in mice

Therapy with IM-250 had no effect on the weight of mice. In a pharmacokinetic study of uninfected mice ($n = 3$) fed with the 150 mg/kg containing diet for 7 days, the mean total plasma concentrations were 6.6, 5.8, 6.3, 7.8 and 5.6 μM on day 1, 2, 3, 5 and 7, respectively. After treatment (by changing the diet to standard chow) the plasma concentrations of IM-250 dropped to 0.5, 0.035, 0.022 and 0.007 μM on days 8, 9, 10 and 12, respectively.

3.2. Results of the guinea pig experiments

3.2.1. Recurrent disease

The guinea pig model mimics genital herpes in humans, including development of latency and recurrent disease (Bernstein, 2020). For evaluation of recurrent infections, guinea pigs were infected with HSV-2 and the acute disease left untreated. After latency developed, therapy was initiated as intermittent treatment during the recurrent disease period to evaluate drug efficacy on recurrent infection, the frequency of recurrent disease and the reactivation competence of the latent neuronal viral reservoir. As shown in Fig. 1A and B, recurrent mean cumulative lesions scores were reduced by both IM-250 and ACV (0.9 ± 1.0 and 3.0 ± 2.1 respectively, versus 3.9 ± 3.2 in the no treatment group) but only the IM-250 group difference was significant with ($P < 0.001$). IM-250 treated animals also had significantly fewer recurrences compared to the ACV group, ($P < 0.05$). Similarly, the number of animals that were recurrence free during the entire duration of follow-up was significantly ($P < 0.05$) greater in the IM-250 group ($n = 7$) than either of the other groups ($n = 1$) (Fig. 1C).

In an attempt to further understand the persistent effects of IM-250 we next compared the recurrent lesion days in the off periods (when animals were receiving chow and water without any treatments). We found that only the IM-250 group (0.7 ± 0.8) had reduced recurrences compared to vehicle (1.81 ± 2.0; $P = 0.09$) or ACV (2.0 ± 1.6; $P < 0.05$) during these off treatment periods (Fig. 2A). Note that as expected, ACV had no effect during these periods compared to vehicle. After 7 cycles (week 15) there were no further recurrences in the IM-250 treated group while the other 2 groups continued to develop recurrences (**$P < 0.005$ versus ACV, $P = 0.15$ versus vehicle (Fig. 2B).

3.2.2. Latent virus

The results of the qPCR evaluations revealed only a small and not significant reduction in latent HSV-2 DNA (−11.7% in dorsal root ganglia (DRG) and −6.3% in spinal cord (SC)) in the IM-250 treated groups. As shown in Fig. 3, the viral load in the DRG (Fig. 3A, 2.23 ± 1.09 versus 2.17 ± 1.11 Mean Log_{10} HSV-2 copies/μg of DNA) and SC

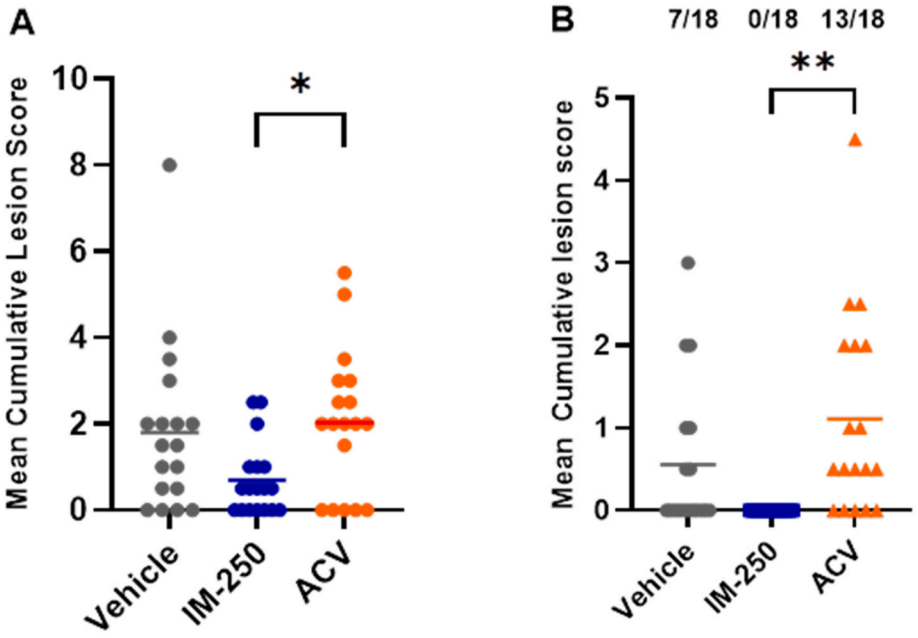

Fig. 2. Evidence that IM-250 has persistent effects on reactivatable virus.
HSV-2 infected guinea pigs were randomized after latency was established to receive twelve cycles of 7 days on and 7 days off therapy (over 6 months). (**A**) Comparison of recurrent lesion scores in all the off periods (i.e. when animals are on standard food and drink) shows reduction of cumulative lesion score in the IM-250 group versus ACV (*$P < 0.05$) treated groups. (**B**) After 7 cycles of treatment have been completed none of the IM-250 treated animals show recurrent disease compared to ACV (**$P < 0.005$) treated groups.

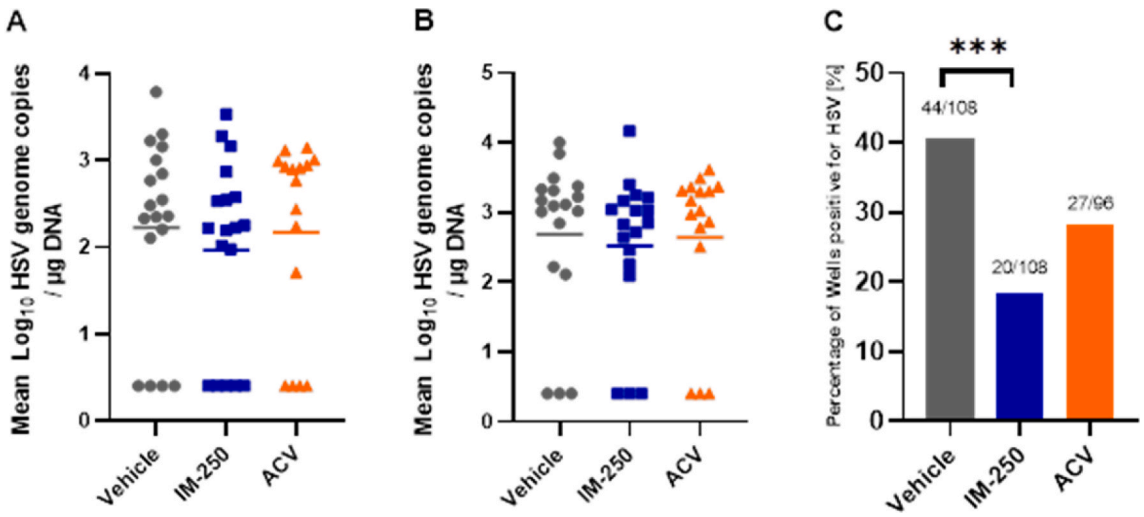

Fig. 3. Latent virus load and HSV-2 reactivation competence after therapy is completed.
HSV-2 infected guinea pigs received twelve cycles of 7 days on and 7 days off therapy (over 6 months). After therapy was completed animals were sacrificed and the dorsal root ganglia (DRG) and spinal cord (SC) were removed and evaluated for latent virus by qPCR and explant co-cultivation. (**A**) and (**B**) Small reduction of HSV-2 genome copy number by qPCR in DRG (**A**) and SC (**B**) of IM-250 treated animals. (**C**) Reduced number of cultures positive for HSV-2 reactivation in the IM-250 treated group versus Vehicle (***$P < 0.001$) and ACV (fewer samples were obtained from the ACV group, because of a loss of 2 animals before the conclusion of the experiment).

(Fig. 3B, 2.69 ± 1.15 versus 2.64 ± 1.15 Mean Log_{10} HSV-2 copies/µg of DNA) was similar for vehicle and ACV treated groups, respectively, in the study, with the lowest viral load observed in the groups receiving IM-250 (Fig. 3A, 1.97 ± 1.08 and Fig. 3B, 2.52 ± 1.08 Mean Log_{10} HSV-2 copies/µg of DNA). However, when examined for reactivatable virus using explant cultures there was a significant reduction in the number of wells where HSV-2 was detected (19% of IM-250 versus 41% of controls, $P < 0.001$ and 28% of ACV, $P = 0.13$) (Fig. 3C).

3.3. Results of the mouse experiments

Latently infected mice were first treated with a single dose of IM-250 (10 mg/kg) just prior to HS to demonstrate that the latent reporter virus effectively marked initiation of reactivation while production of HSV-1

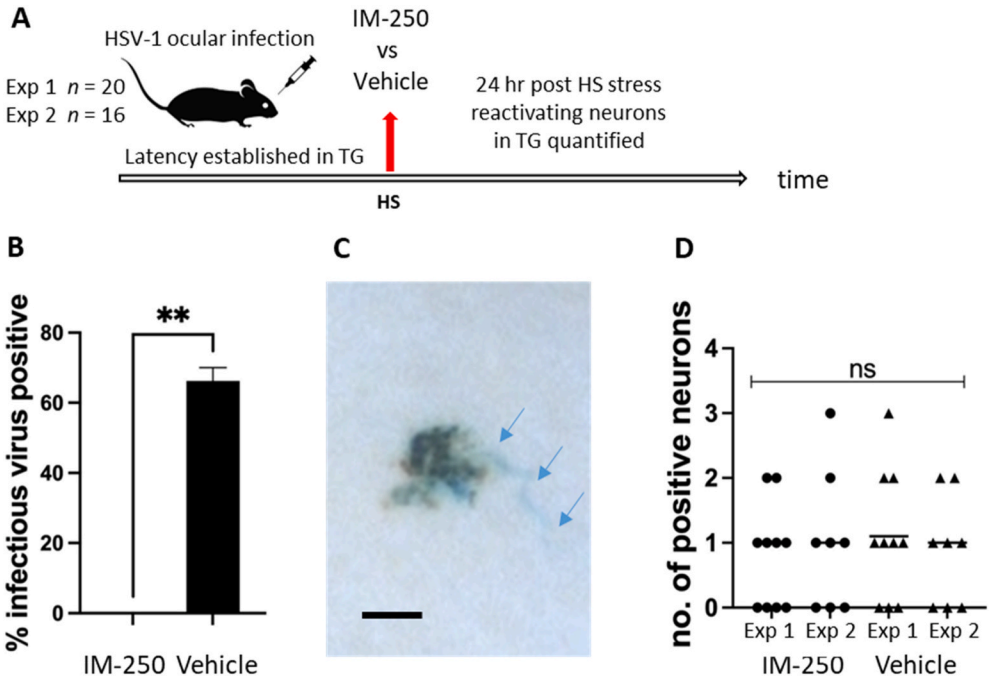

Fig. 4. Analysis of trigeminal ganglia (TG) after single treatment.
The mouse HSV-1 ocular model was utilized to test the effect of IM-250 treatment on HSV-1 induced *in vivo* reactivation and reactivation competency. (**A**) Latently infected mice were treated with IM-250 (10 mg/kg) or vehicle 3 h prior to hyperthermic stress (HS), sacrificed 24 h post HS and the number of neurons exiting latency was quantified. (**B**) IM-250 treatment blocked significantly (**$P = 0.003$) infectious virus production (full reactivation) in 100% of mice (combined data from 2 separate experiments of $n = 10$ and $n = 8$). (**C**) Photomicrograph of neuron in TG that has exited latency. Both x-gal staining (blue, indicating lytic promoter activity) and viral protein (brown, HRP/DAB staining) are shown. Arrows indicate x-gal staining in axon. Bar = 50 µm. (**D**) Quantification of the number of neurons exiting latency in IM-250 and vehicle treated mice revealed no significant difference.

was fully blocked (Fig. 4). Utilizing a single oral treatment prior to reactivation (Fig. 4A), IM-250 blocked viral reactivation (infectious virus production) in 100% of mice in two independent experiments. Infectious virus was not detected in treated (0/10 and 0/8 TG) versus non-treated mice in which 7/10 and 5/8 TG were positive for infectious virus (Fig. 4B, $P = 0.003$). Further details of the experimental design for mouse experiments are presented in section 2.6.

IM-250 treatment did not block VP16p driven β-gal activity or viral protein expression associated with the aborted lytic cycle induced by HS (Fig. 4C). The number of viral protein positive neurons in treated compared to vehicle treated was not different in two independent experiments (Fig. 4D, $P = 0.89$, one-way ANOVA). Thus, a single treatment with IM-250 did not eliminate the aborted lytic cycle entry or the ability to detect individual neurons in the latent pool that are entering the viral lytic but did prevent detectable levels of infectious virus (Sawtell et al., 2006). These data serve as the baseline for the multiple treatment cycles below (Fig. 5).

Intermittent IM-250 treatment was next evaluated to test the effect of multiple treatment cycles on the reactivation competency of the latent reservoir (Fig. 5A). The number of neurons undergoing reactivation, i.e. expressing the lytic cycle marker/proteins in each group was quantified in two independent experiments. Both experiments showed a startling reduction in the number of neurons undergoing reactivation in the IM-250 treated groups compared to the vehicle control groups (Fig. 5B and C). In the first smaller experiment, no neurons undergoing reactivation were detected in TG ($n = 8$) from mice that received intermittent IM-250 therapy, while a total of 15 neurons undergoing reactivation were detected in TG ($n = 8$) from the vehicle treated mice (Fig. 5B, $^{**}P = 0.0083$). In the second larger experiment, a 3.6-fold reduction in total neurons undergoing reactivation in prior IM-250 treated (24 TG) versus vehicle control (24 TG) was observed (Fig. 5C, $^{**}P = 0.0025$). When these two experiments were combined, the latent reservoirs (TG) from mice previously exposed to IM-250 during hyperthermic stress induced reactivation yielded a total of only 8 neurons compared to 44 in the vehicle treated reservoirs. Thus, prior intermittent treatment with IM-250 in some way altered the latent reservoir such that when exposed to a reactivation stressor, the number of individual neurons undergoing reactivation in the collective latent reservoir of treated mice was reduced by nearly 550% compared to the number in the reservoir of vehicle-treated control mice. (Fig. 5D). Fig. 5E and F show an example of a neuron undergoing reactivation in the TG at low (E) and high (F) magnification.

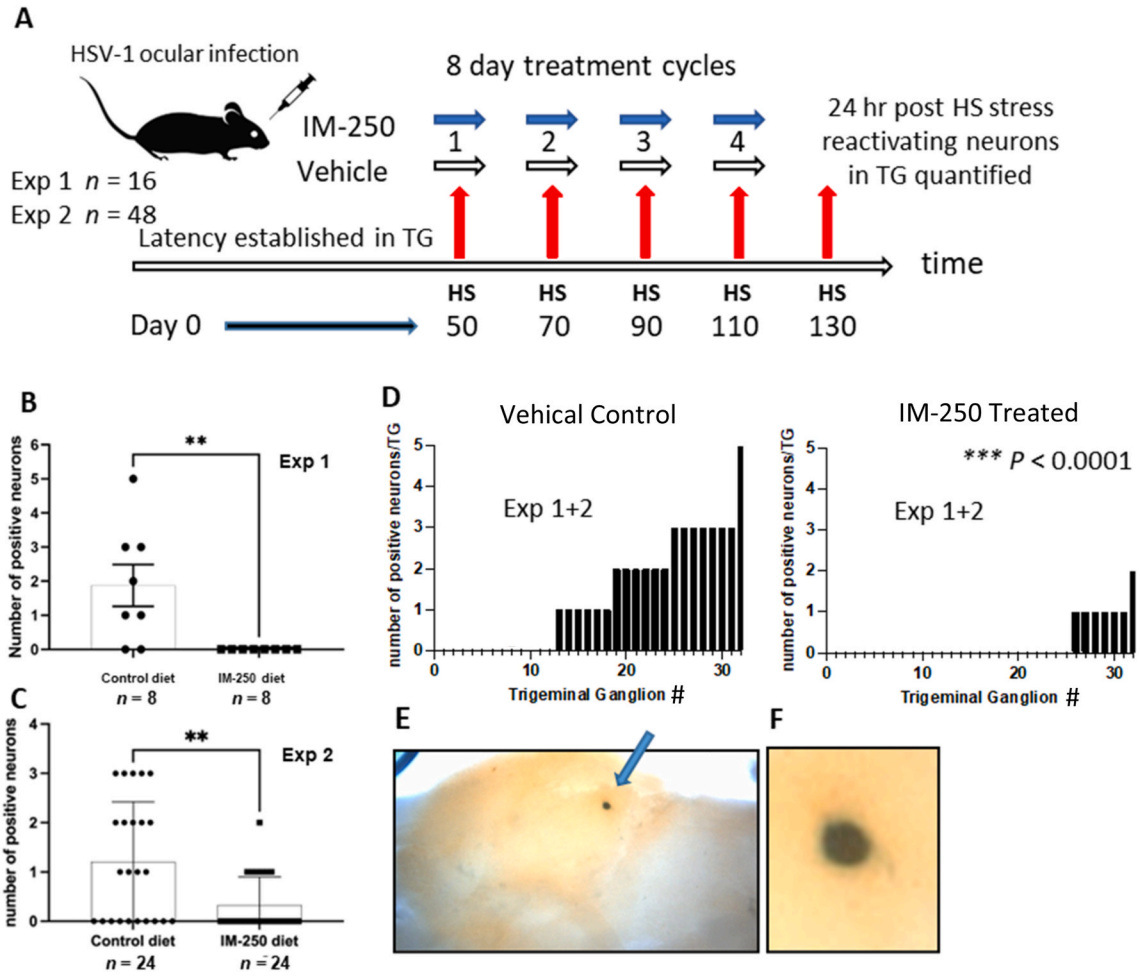

Fig. 5. Reactivation competency in latent reservoir following intermittent vehicle or IM-250 treatment.
The mouse HSV-1 ocular model was utilized to test the effect of IM-250 treatment on HSV-1 induced *in vivo* reactivation and reactivation competency. (**A**) Intermittent IM-250 treatment was delivered in chow according to the schedule shown. Mice were subjected to HS at the midpoint of each of 4 treatment cycles. Thirteen days after the last cycle of IM-250, mice received a final hyperthermic stress and 24 h later reactivation competency (the total number of neurons exiting latency in the TG) was quantified. (**B**) and (**C**) The number of neurons exiting latency (competent to reactivate) was significantly ($^{**}P < 0.01$ (**B**) and (**C**)) reduced in TG from mice intermittently treated with IM-250 compared to vehicle treated in two independent experiments. (**D**) Data combined ($^{***}P < 0.0001$) from both experiments emphasizing the dramatic reduction in reactivation competency between vehicle control (left panel) and IM-250 treated (right panel) groups. (**E**) Photomicrograph of whole mount TG from the vehicle group showing neuron exiting latency (arrow) and (**F**) shown at higher magnification.

The mechanism underlying this reduced reactivation *in vivo* is not known but of great interest. A first possibility is increased inflammation and destruction of neurons with IM-250 treatment during the prior reactivation cycles. To test this, ganglia from each reactivation group were additionally processed after whole ganglion analysis and sectioned for histological examination as detailed in methods. Representative sections from intermittent vehicle and IM-250 treated TG are shown in Fig. 6A,a, B,b. The number of neurons counted in each of 10 fields selected from 5 TG from each group were not different (61.1 (range 50–75) and 60.9 (range 46–71)) in IM-250 and vehicle control groups, respectively (Fig. 6C, $P = 0.95$). This suggests that extensive neuronal drop out is not the explanation. Sectioned TG were also examined for inflammatory foci associated with HSV reactivation (Sawtell and Thompson, 1992, 2021; Doll et al., 2020). As shown in Fig. 6D, characteristic clusters of cells accumulating in foci at the site of a reactivating neuron are observed in TG from vehicle-treated but not the IM-250 treated group Fig. 6B. These cells have been characterized previously as Iba1-expressing cells (Doll et al., 2020) and associated with sites of HSV reactivation in the TG (Fig. 6D and E). Importantly, we found no evidence of increased inflammation or tissue destruction in the IM-250 treated group Fig. 6B.

4. Discussion

Currently, herpes simplex infections are predominantly treated with generic nucleosidic drugs such as acyclovir, valacyclovir, penciclovir and famciclovir (Kleymann, 2005; De Clercq and Li, 2016). Second line treatment utilizes drugs that are associated with significant side effects such as foscarnet, brivudine and cidofovir (Kleymann, 2005; De Clercq and Li, 2016; Workowski and Bolan, 2015; Sadowski et al., 2021). These therapies have several shortcomings including only partial effects on transmission (Corey et al., 2004; Mujugira et al., 2013) and the emergence of resistant viruses especially in immunocompromised patients (Piret and Boivin, 2016). Significantly there is no current therapy that affects latent virus nor the risk, frequency, or severity of recurrences after the drug is discontinued (Piret and Boivin, 2016; Wald et al., 1994) (https://www.cdc.gov/std/treatment-guidelines/herpes.htm). Thus, life-long therapy is necessary to control recurrences. Further, owing to their poor CNS penetration, therapy is only modestly effective for the most serious HSV diseases, neonatal HSV (Pinninti and Kimberlin, 2018; Thompson and Whitley, 2011) and HSV encephalitis (Gnann and Whitley, 2017). This lack of CNS exposure also raises the question whether these drugs would have an impact on CNS diseases, such as Alzheimer's disease, if indeed herpes virus plays a role in these diseases (Harris and Harris, 2015; Itzhaki and Lathe, 2018).

In a recent article (Gege et al., 2021), we presented the preclinical profile of IM-250 and showed that treatment of primary infection of vaginally HSV-infected guinea pigs with IM-250 completely prevented initial infection and significantly decreased the latent neuronal viral reservoir. Furthermore, treatment of latently infected animals reduced recurrent disease, and the number of days with lesions and viral shedding thus increasing the number of disease free animals on and off therapy. In the studies presented here, we provide compelling evidence generated from two classic HSV latency/reactivation models that intermittent treatment with IM-250 alters the latent viral reservoir in such a way that reactivation is significantly reduced.

The guinea pig is the most commonly used small animal model in which spontaneous recurrences develop allowing prolonged observations of natural recurrent disease (Bernstein, 2020). In guinea pigs there were several analyses that suggest that IM-250 therapy affected reactivatable virus after several rounds of intermittent therapy: 1) therapy decreased recurrences during the no treatment weeks as well as during therapy, 2) after 7 cycles there were no further recurrences during either the treatment or no treatment weeks, and 3) explant reactivation events were significantly less in the IM-250 treated group.

These data are significantly enhanced in the mouse model as there is an in depth understanding of key relationships between latent viral genome copy number profile and reactivation competency ((Sawtell, 1998; Sawtell, 2003), reviewed in (Sawtell and Thompson, 2021)). The impressive stability of the latent reservoir with respect to the number of latently infected neurons and the distribution of viral genome copies in these neurons as well as the documented reactivation competency in this model is ideally suited to test the hypothesis that intermittent IM-250 treatment alters the *in vivo* reactivation competency of the established latent reservoir. The reduction in reactivation competent neurons by 550% over a span of only 4 induced reactivation/IM-250 treatment events is startling. This suggests that the mechanism(s) required for maintaining or producing reactivation competent neurons has been disrupted. While little is known about this aspect of HSV biology, the latency associated transcript (LAT) locus has been shown to play a role in the maintenance of the viral genome over time (Thompson and Sawtell, 2011).

Our current working hypothesis is that the few neurons bearing high HSV genome copies (e.g. > 10000 episomal HSV genomes) that are reactivation competent (Sawtell and Thompson, 2021; Sawtell, 1998; Sawtell et al., 1998) *in vivo* are affected by intermittent IM-250 therapy. This would account for the lack of significant decreases in overall genome copy number and yet a profound effect on reactivation as

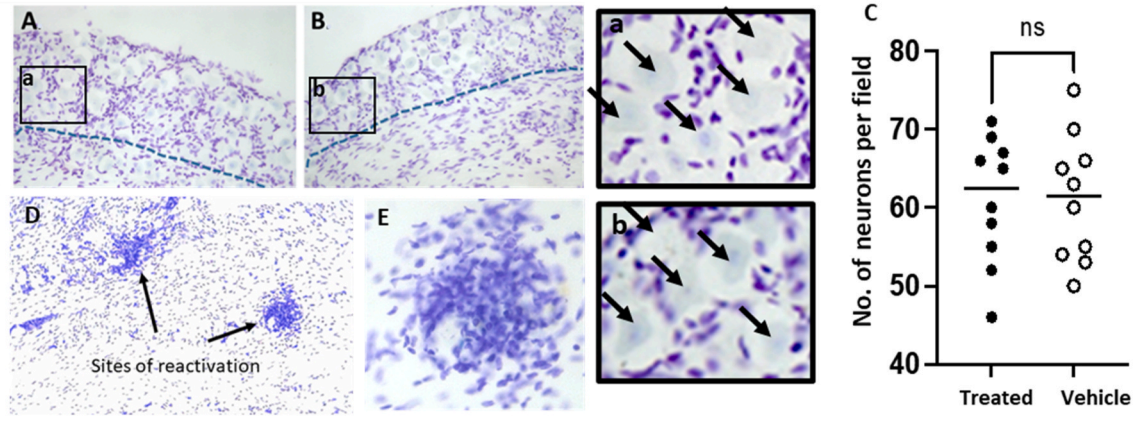

Fig. 6. Histological examination of mouse trigeminal ganglia (TG) post stress.
Photomicrographs of cresyl violet stained sections of trigeminal ganglia post final stress. Examination of sectioned TG from intermittently vehicle (**A**) or IM-250 (**B**) treated groups revealed no difference in the overall number of neurons in the ganglia (**C**, ns = not significant). Higher power views of neurons in boxed areas are shown in (**a**) and (**b**), arrows indicate neurons. Reactivation related inflammatory foci observed in vehicle control [(**D**) arrows, and (**E**) at higher magnification] were not detected in the IM-250 treated TG examined (B).

assessed by explants in guinea pigs and induced *in vivo* reactivation in mice. To elaborate, we note that mean HSV genome copy numbers were consistently lower in DRG but only by −11.7 to −20.0% (0.26–0.42 Log_{10} HSV copies/μg of DNA) and in SC by −6.3% to −17.2% (0.17–0.45 Log_{10} HSV copies/μg of DNA) in the intermittently IM-250 treated groups compared to no treatment or ACV in both the present experiment and the published work (Gege et al., 2021). Thus, the overall decrease would not account for the much larger decrease in reactivation leading us to hypothesize that the effects are more likely restricted to reactivation competent neurons. We believe that the increased CNS penetration and high neuronal concentrations of IM-250 could limit HSV replication and local neuronal spread that leads to high copy numbers in neurons that reactivate. The duration of protection from reactivation is an important outcome that will be studied in clinical trials but even if the silencing of recurrences is not permanent and the pool of reactivable virus is replenished over time, a brief respite from recurrences would be beneficial and may be enhanced by periodically treatment.

The PK data obtained from experimental animals indicate that the drug levels were well above the EC_{50} during therapy but did not exceed toxic levels (Gege et al., 2021). Harvesting of ganglia and scoring during the off treatment period started, when free drug concentrations would be below the IC_{50} ruling out effects of residual drug effects during analysis. Results of animal models may not necessarily translate into humans, however, silencing of recurrences by IM-250 therapy was demonstrated with two human HSV strains (HSV-1 and HSV-2) in two animal models with natural HSV recurrences (guinea pig model) and controlled hyperthermic stress (mouse model) at least twice each.

The major limitation of the guinea pig study is the use of ACV as the comparator groups as ACV is less effective in guinea pigs than humans due to its shorter half-life (Good and de Miranda, 1982). However, this drug is the most commonly used treatment and has been previously used as a control for guinea pig experiments (Bernstein et al., 2015; Baumeister et al., 2007, Katsumata et al., 2011). The lower exposure of ACV in nerve cells and the different mechanism of action compared to the helicase-primase inhibitor IM-250 may be the basis why in contrast to ACV IM-250 reduces future reactivation from the latent viral reservoir.

In conclusion, IM-250 shows great promise as a treatment for both oral and genital HSV infections and appears to alter the paradigm that latent HSV infections cannot be affected by antiviral therapies. Further, the increased CNS penetration should provide improved therapies for neonatal and encephalitic disease. The mechanism of action for the effect on latent virus is an area of intense interest and under investigation. Phase 1 clinical trials to investigate the safety, tolerability and pharmacokinetics of IM-250 have started in 2023.

Funding

This research did not receive any specific grant from funding agencies in the public, commercial, or not-for-profit sectors.

Author contributions

CG and GK invented IM-250. CG and GK planned synthesis routes and organized production of compounds. DIB, FJB, and GK planned and analyzed guinea pig animal experiments statistically. FJB and DAD performed the guinea pig experiments including processing of the animal samples. NMS and GK planned the mouse experiments and NMS performed and analyzed the animal experiments statistically. DIB, NMS and GK organized experiments and wrote the manuscript. All authors contributed to the final manuscript, figures, and tables.

Declaration of competing interest

The authors declare the following financial interests/personal relationships which may be considered as potential competing interests: CG and GK are inventors of patent families WO2017/174640 (Title: Aminothiazole derivatives useful as antiviral agents) and WO2019/068817 (Title: Enantiomers of substituted thiazoles as antiviral compounds). DIB is a consultant to Innovative Molecules GmbH. All other authors declare that they have no competing interests.

Data availability

Data will be made available on request.

Acknowledgements

We thank Richard L. Thompson for providing HSV-1 virus 17VP16pLZ for use in the mouse studies.

Glossary

ACV	Acyclovir
ANOVA	Analysis of variance
CNS	Central nervous system
DMSO	Dimethyl sulfoxide
DNA	Deoxyribonucleic acid
DRG	Dorsal root ganglia
EC_{50}	Half maximal effective concentration
HFBA	Heptafluorobutyric acid
HPI	Helicase-primase inhibitor
HPMC	Hydroxypropyl methylcellulose
HRP/DAB	Horseradish peroxidase/3,3′-diaminobenzidine
HS	Hyperthermic stress
HSV(-1)	Herpes simplex virus (-type 1)
HSV(-2)	Herpes simplex virus (-type 2)
IC_{50}	Half maximal inhibitory concentration
IM-250	(*S*)-2-(2′,5′-Difluoro-[1,1′-biphenyl]-4-yl)-*N*-methyl-*N*-(4-(methyl-d_3)-5-(*S*-methyl sulfonimidoyl)thiazol-2-yl) acetamide
LAT	Latency associated transcript
LC-MS/MS	Liquid chromatography with tandem mass spectrometric detection
NOAEL	No-observed-adverse-effect level
PBS	Phosphate buffered saline
qPCR	Quantitative polymerase chain reaction
RSC	Rabbit skin cell
SC	Spincal cord
TG	Trigeminal ganglia
x-gal	5-Bromo-4-chloro-3-indolyl-β-D-galactopyranoside

References

Bacon, T.H., Levin, M.J., Leary, J.J., Sarisky, R.T., Sutton, D., 2003. Herpes simplex virus resistance to acyclovir and penciclovir after two decades of antiviral therapy. Clin. Microbiol. Rev. 16, 114–128. https://doi.org/10.1128/cmr.16.1.114-128.2003.

Baumeister, J., Fischer, R., Eckenberg, P., Henninger, K., Ruebsamen-Waigmann, H., Kleymann, G., 2007. Superior efficacy of helicase-primase inhibitor BAY 57-1293 for herpes infection and latency in the Guinea pig model of human genital herpes disease. Antivir. Chem. Chemother. 18, 35–48. https://doi.org/10.1177/0956320207018001.

Bernstein, D.I., 2020. Use of the Guinea pig model of genital herpes to evaluate vaccines and antivirals: review. Antivir. Res. 180, 104821 https://doi.org/10.1016/j.antiviral.2020.104821.

Bernstein, D.I., Bravo, F.J., Pullum, D.A., Shen, H., Wang, M., Rahman, A., Glazer, R.I., Cardin, R.D., 2015. Efficacy of *N*-methanocarbathymidine against genital herpes simplex virus type 2 shedding and infection in Guinea pigs. Antivir. Chem. Chemother. 24, 19–27. https://doi.org/10.1177/2040206614566581.

Bernstein, D.I., Cardin, R.D., Smith, G.A., Pickard, G.E., Sollars, P.J., Dixon, D.A., Pasula, R., Bravo, F.J., 2020. The R2 non-neuroinvasive HSV-1 vaccine affords protection from genital HSV-2 infections in a Guinea pig model. NPJ Vaccines 5, 104. https://doi.org/10.1038/s41541-020-00254-8.

Bourne, N., Stanberry, L.R., Kern, E.R., Holan, G., Matthews, B., Bernstein, D.I., 2000. Dendrimers, a new class of candidate topical microbicides with activity against herpes simplex virus infection. Antimicrob. Agents Chemother. 44, 2471–2474. https://doi.org/10.1128/aac.44.9.2471-2474.2000.

Bryson, Y.J., Dillon, M., Lovett, M., Acuna, G., Taylor, S., Cherry, J.D., Johnson, B.L., Wiesmeier, E., Growdon, W., Creagh-Kirk, T., Keeney, R., 1983. Treatment of first

episodes of genital herpes simplex virus infection with oral acyclovir – a randomized double-blind controlled trial in normal subjects. N. Engl. J. Med. 308, 916–921. https://doi.org/10.1056/nejm198304213081602.

Corey, L., Wald, A., Patel, R., Sacks, S.L., Tyring, S.K., Warren, T., Douglas Jr., J.M., Paavonen, J., Morrow, R.A., Beutner, K.R., Stratchounsky, L.S., Mertz, G., Keene, O. N., Watson, H.A., Tait, D., Vargas-Cortes, M., 2004. Valacyclovir HSV Transmission Study Group, Once-daily valacyclovir to reduce the risk of transmission of genital herpes. N. Engl. J. Med. 350, 11–20. https://doi.org/10.1056/nejmoa035144.

De Clercq, E., Li, G., 2016. Approved antiviral drugs over the past 50 years. Clin. Microbiol. Rev. 29, 695–747. https://doi.org/10.1128/cmr.00102-15.

Doll, J.R., Hoebe, K., Thompson, R.L., Sawtell, N.M., 2020. Resolution of herpes simplex virus reactivation in vivo results in neuronal destruction. PLoS Pathog. 16, e1008296 https://doi.org/10.1371/journal.ppat.1008296.

Gege, C., Bravo, F.J., Uhlig, N., Hagmaier, T., Schmachtenberg, R., Elis, J., Burger-Kentischer, A., Finkelmeier, D., Hamprecht, K., Grunwald, T., Bernstein, D.I., Kleymann, G., 2021. A helicase-primase drug candidate with sufficient target tissue exposure affects latent neural herpes simplex virus infections. Sci. Transl. Med. 13, eabf8668 https://doi.org/10.1126/scitranslmed.abf8668.

Gnann Jr., J.W., Whitley, R.J., 2017. Herpes simplex encephalitis: an update. Curr. Infect. Dis. Rep. 19, 13. https://doi.org/10.1007/s11908-017-0568-7.

Good, S.S., de Miranda, P., 1982. Metabolic disposition of acyclovir in the Guinea pig, rabbit, and monkey. Am. J. Med. 73, 91–95. https://doi.org/10.1016/0002-9343(82)90071-7.

Harris, S.A., Harris, E.A., 2015. Herpes simplex virus type 1 and other pathogens are key causative factors in sporadic Alzheimer's disease. J. Alzheim. Dis. 48, 319–353. https://doi.org/10.3233/2FJAD-142853.

Itzhaki, R.F., Lathe, R., 2018. Herpes viruses and senile dementia: first population evidence for a causal link. J. Alzheim. Dis. 64, 363–366. https://doi.org/10.3233/jad-180266.

James, C., Harfouche, M., Welton, N.J., Turner, K.M.E., Abu-Raddad, L.J., Gottlieb, S.L., Looker, K.J., 2020. Herpes simplex virus: global infection prevalence and incidence estimates, 2016. Bull. World Health Organ. 98, 315–329. https://doi.org/10.2471/blt.19.237149.

Katsumata, K., Chono, K., Sudo, K., Shimizu, Y., Kontani, T., Suzuki, H., 2011. Effect of ASP2151, a herpesvirus helicase-primase inhibitor, in a guineapig model of genital herpes. Molecules 16, 7210–7223. https://doi.org/10.2471/blt.19.237149.

Kawashima, M., Watanabe, D., Fujio, K., Komazaki, H., 2023. A phase 3, randomized, double-blind, placebo-controlled study evaluating a single, patient initiated dose of amenamevir for recurrent herpes labialis. J. Dermatol. 50, 311–318. https://doi.org/10.1111/1346-8138.16608.

Kleymann, G., 2005. Agents and strategies in development for improved management of herpes simplex virus infection and disease. Expet Opin. Invest. Drugs 14, 135–161. https://doi.org/10.1517/13543784.14.2.135.

Kleymann, G., Gege, C., 2017. Aminothiazole Derivatives Useful as Antiviral Agents. WO2017/174640.

Kleymann, G., Gege, C., 2019. Enantiomers of Substituted Thiazoles as Antiviral Compounds. WO2019/068817.

Mujugira, A., Magaret, A.S., Celum, C., Baeten, J.M., Lingappa, J.R., Morrow, R.A., Fife, K.H., Delany-Moretlwe, S., de Bruyn, G., Bukusi, E.A., Karita, E., Kapiga, S., Corey, L., Wald, A., for the Partners in Prevention HSV/HIV Transmission Study Team, 2013. Daily acyclovir to decrease herpes simplex virus type 2 (HSV-2) transmission from HSV-2/HIV-1 coinfected persons: a randomized controlled trial. J. Infect. Dis. 208, 1366–1374. https://doi.org/10.1093/2Finfdis/2Fjit333.

Pinninti, S.G., Kimberlin, D.W., 2018. Neonatal herpes simplex virus infections. Semin. Perinatol. 42, 168–175. https://doi.org/10.1053/j.semperi.2018.02.004.

Piret, J., Boivin, G., 2016. Antiviral resistance in herpes simplex virus and varicella-zoster virus infections: diagnosis and management. Curr. Opin. Infect. Dis. 29, 654–662. https://doi.org/10.1097/qco.0000000000000288.

Sadowski, L.A., Upadhyay, R., Greeley, Z.W., Margulies, B.J., 2021. Current drugs to treat infections with herpes simplex viruses-1 and -2. Viruses 13, 1228. https://doi.org/10.3390/v13071228.

Sawtell, N.M., 1998. The probability of in vivo reactivation of herpes simplex virus type 1 increases with the number of latently infected neurons in the ganglia. J. Virol. 72, 6888–6892. https://doi.org/10.3390/v13071228.

Sawtell, N.M., 2003. Quantitative analysis of herpes simplex virus reactivation in vivo demonstrates that reactivation in the nervous system is not inhibited at early times postinoculation. J. Virol. 77, 4127–4138. https://doi.org/10.1128/jvi.77.7.4127-4138.2003.

Sawtell, N.M., 2005. Detection and quantification of the rare latently infected cell undergoing herpes simplex virus transcriptional activation in the nervous system in vivo. Methods Mol. Biol. 292, 57–71. https://doi.org/10.1385/1-59259-848-x:057.

Sawtell, N.M., Thompson, R.L., 1992. Rapid in vivo reactivation of herpes simplex virus in latently infected murine ganglionic neurons after transient hyperthermia. J. Virol. 66, 2150–2156. https://doi.org/10.1128/2Fjvi.66.4.2150-2156.1992.

Sawtell, N.M., Thompson, R.L., 2020. HSV mutant generation and dual detection methods for gaining insight into latent/lytic cycles in vivo. Methods Mol. Biol. 2060, 219–239. https://doi.org/10.1007/978-1-4939-9814-2_12.

Sawtell, N.M., Thompson, R.L., 2016. De novo herpes simplex virus VP16 expression gates a dynamic programmatic transition and sets the latent/lytic balance during acute infection in trigeminal ganglia. PLoS Pathog. 12 (9), e1005877 https://doi.org/10.1371/journal.ppat.1005877.

Sawtell, N.M., Thompson, R.L., 2021. Alphaherpesvirus latency and reactivation with a focus on herpes simplex virus. Curr. Issues Mol. Biol. 41, 267–356. https://doi.org/10.21775/cimb.041.267.

Sawtell, N.M., Poon, D.K., Tansky, C.S., Thompson, R.L., 1998. The latent herpes simplex virus type 1 genome copy number in individual neurons is virus strain specific and correlates with reactivation. J. Virol. 72, 5343–5350. https://doi.org/10.1128/2Fjvi.72.7.5343-5350.1998.

Sawtell, N.M., Thompson, R.L., Haas, R.L., 2006. Herpes simplex virus DNA synthesis is not a decisive regulatory event in the initiation of lytic viral protein expression in neurons in vivo during primary infection or reactivation from latency. J. Virol. 80, 38–50. https://doi.org/10.1128/2FJVI.80.1.38-50.2006.

Stanberry, L.R., Kern, E.R., Richards, J.T., Abbott, T.M., Overall Jr., J.C., 1982. Genital herpes in Guinea pigs: pathogenesis of the primary infection and description of recurrent disease. J. Infect. Dis. 146, 397–404. https://doi.org/10.1093/infdis/146.3.397.

Thompson, R.L., Sawtell, N.M., 2011. The herpes simplex virus type 1 latency associated transcript locus is required for the maintenance of reactivation competent latent infections. J. Neurovirol. 17, 552–558. https://doi.org/10.1007/s13365-011-0071-0.

Thompson, C., Whitley, R., 2011. Neonatal herpes simplex virus infections: where are we now? Adv. Exp. Med. Biol. 697, 221–230. https://doi.org/10.1007/2F978-1-4419-7185-2_15.

Thompson, R.L., Preston, C.M., Sawtell, N.M., 2009. De novo synthesis of VP16 coordinates the exit from HSV latency in vivo. PLoS Pathog. 5, e1000352 https://doi.org/10.1371/journal.ppat.1000352.

Uhlig, N., Donner, A.-K., Gege, C., Lange, F., Kleymann, G., Grunwald, T., 2021. Helicase primase inhibitors (HPIs) are efficacious for therapy of human herpes simplex virus (HSV) disease in an infection mouse model. Antivir. Res. 195, 105190 https://doi.org/10.1016/j.antiviral.2021.105190.

Wald, A., Benedetti, J., Davis, G., Remington, M., Winter, C., Corey, L., 1994. A randomized, double-blind, comparative trial comparing high- and standard-dose oral acyclovir for first-episode genital herpes infections. Antimicrob. Agents Chemother. 38, 174–176. https://doi.org/10.1128/aac.38.2.174.

Wald, A., Corey, L., Timmler, B., Magaret, A., Warren, T., Tyring, S., Johnston, C., Kriesel, J., Fife, K., Galitz, L., Stoelben, S., Huang, M.-L., Selke, S., Stobernack, H.-P., Ruebsamen-Schaeff, H., Birkmann, A., 2014. Helicase-primase inhibitor pritelivir for HSV-2 infection. N. Engl. J. Med. 370, 201–210. https://doi.org/10.1056/nejmoa1301150.

Workowski, K.A., Bolan, G.A., 2015. Sexually transmitted diseases treatment guidelines, 2015. Morb. Mortal. Wkly. Rep. 64, 1–137. https://www.cdc.gov/mmwr/preview/mmwrhtml/rr6403a1.htm.